

# Influence of hydrogen bond networks in Glycerol / N-Methyl-2-Pyrrolidone mixtures studied by dielectric relaxation spectroscopy



V Manjula<sup>a,b</sup>, T. Vamshi Prasad<sup>c</sup>, K Balakrishna<sup>a</sup>, K. C. James Raju<sup>d,\*</sup>, T Vishwam<sup>a,\*</sup>

<sup>a</sup> Department of Physics and Chemistry, GITAM (Deemed to be University), Hyderabad, Rudraram, Patancheru (M), Telangana, 502329, India

<sup>b</sup> Department of Physics Geethanjali College of Engineering and Technology, Hyderabad, Telangana 501301, India

<sup>c</sup> Department of Physics, Jawaharlal Nehru Technological University, Hyderabad, Hyderabad, 500 085, India

<sup>d</sup> School of Physics, University of Hyderabad, Hyderabad, Telangana 500046, India

## ARTICLE INFO

### Article history:

Received 5 October 2020

Revised 23 November 2020

Accepted 29 November 2020

Available online 4 December 2020

### Keywords:

Dielectric permittivity

Relaxation

Excess parameters

Mean molecular polarizability

Activation energies

## ABSTRACT

In this paper, we report the dielectric permittivity of the Glycerol (Gly) with N-Methyl-2-Pyrrolidone (NMP) binary mixtures in the microwave frequency region at different temperatures. The dipole moments of Gly, NMP and their equimolar binary mixtures are calculated by using Higasi's method in the temperature range 298.15K–323.15K. The dielectric relaxation spectra of the binary mixtures are calculated using Cole-Cole and Cole-Davidson equation and shows an unsymmetrical relaxation behaviour. The excess parameters of volume, permittivity, refractive index, polarization and relaxation times are fitted with Redlich-Kister polynomial equation. The molecular association and their hydrogen bond interactions between the components in the mixture are discussed in terms of Kirkwood correlation  $g^{eff}$  factor and excess Helmholtz energy ( $\Delta F^E$ ) equation. The mean molecular polarizability ( $\alpha_M$ ) of the individual and their binary mixture are calculated using Lippincott  $\delta$ -function potential model and compared with the LeFevre method of polarizability values. The enthalpy of activation  $\Delta H^*$ , entropy of activation  $\Delta S^*$  and Gibbs free energy of activation  $\Delta G^*$  are also evaluated and the results are discussed in terms of the orientation of the dipoles. The presence of hydrogen bonding between Gly and NMP is confirmed from the FT-IR spectra.

© 2020 Elsevier B.V. All rights reserved.

## 1. Introduction

The non-destructive characterization of biological samples/liquids, polymers and gels have stimulated the use of dielectric relaxation spectroscopy (DRS) at a broader frequency range at different temperatures [1]. The DRS is one of the sensitive methods to interpret the structural dynamics, molecular association and orientation of the dipoles in the liquid medium [2]. The dielectric relaxation spectroscopy is well suited for to observe the changes in the electrical properties when liquids mix up at different concentrations and also the hydrated studies of proteins/gels with the change in temperature. Therefore, temperature-dependent dielectric relaxation studies of liquid mixtures are of growing interest [3–9]. The investigation of dielectric permittivity of the mixtures by varying concentration of liquid samples helps to ascertain the structure of the complexes formed in the solution

[10–15]. The presence of the hydrogen bond between components present in the mixtures that affect the dielectric permittivity, polarization and its relaxation behaviour properties. The understanding the nature of hydrogen bond remains a complex task due to the type of bonds and components present in the given liquid system [16–22]. The dielectric permittivity studies of hydrogen-bonded polar liquids/polymer nanocomposite materials at broader frequency region are very much interesting and these results are quite useful in the field of biological, medical, and shielding applications [23–32].

Glycerol is a simple polyol compound; due to its antimicrobial and antiviral properties, it is extensively used in wound and burn treatments, effective marker to measure liver diseases, the sweetener in the food industry and as a humectant in pharmaceutical formulations [33–39]. NMP is a good polar solvent with magnificent properties. It is having a wide range of applications due to its higher boiling point, lower freezing point and ease of handling [40,41]. It is used as a solvent for engineering polymers, coating resins, paint stripping, oven cleaners, automotive and industrial cleaner formulations. The dielectric permittivity of the Glyc-

\* Corresponding authors.

E-mail addresses: [kcjrsp@uohyd.ac.in](mailto:kcjrsp@uohyd.ac.in) (K. C.J. Raju), [vitalloju@gitam.edu](mailto:vitalloju@gitam.edu) (T. Vishwam).

erol is measured by Menon Kevin et al. [42] in the frequency range 10<sup>-4</sup> Hz to 20 GHz. Their studies revealed that the imaginary part of the dielectric permittivity depends upon the temperature and their spectra are fitted with Vogel-Fulcher equation to interpret the relaxation behaviour phenomena. Yoshihito Hayashi et al. [43] analysed the relaxation dynamics of Gly-Water mixtures through broadband dielectric spectroscopy in the frequency range 1 Hz-250 MHz and also differential scanning calorimetry study between the temperatures 138-313K. Their result shows that the presence of various types of relaxation process which changes with the concentration of Gly in water mixtures due to its fast and slower dynamics of H-bond structures in the solution. The dielectric characterization of glass-forming Glycerol with varying LiCl salt concentration in the frequency region 20 Hz-3 GHz is studied by Kohler et al. [44] and it is reported that structural dynamics are influenced by the ionic conductivity. The temperature-dependent dielectric constant, viscosity behaviour of Glycerol-amide mixtures are studied by Sengwa et.al [45,46] and the existence of non-local dielectric relaxation phenomena in Glycerol is reported by Pronin et.al [47]. The asymmetrical distribution of relaxation times in Glycerol-water mixtures are well explained by Kaatze et.al [48-50] in terms of hydrogen bond network fluctuations in the system. The concentration dependence of partial molar isobaric expansion of Glycerol- water mixtures were reported by Egorov et al. [51] and the number of hydrogen bonds, binding energies present in the Gly-DMF binary mixtures described by Guo-Zhu Jia et al. [52] using Luzar model. Recently, Yasmine Chabouni et al. [53] studied the temperature-dependent physicochemical properties of the binary mixtures of Glycerol with butanol isomers. Their studies revealed that volumetric, thermal isobaric expansibilities are effectively influenced by the size, shape and position of the hydroxyl group of the components. There are few articles are available in the literature on dielectric studies of NMP with water [54,55], alcohol [56] and DMSO [57] mixtures at one of the specific temperatures 298K but not on Gly-NMP mixtures. The available literature primarily focussed on dielectric studies of mixtures of varying concentrations at one of the temperature but not on temperature-dependent dielectric permittivity, volumetric, thermodynamic properties and polarization studies. This reason motivated us to study the density, volumetric, thermodynamic, molecular polarizability and computational studies (DFT) of Glycerol with NMP binary mixtures.

In the present work, we report the volumetric, dielectric and thermodynamic properties of the Gly /NMP binary mixtures in the temperature range 298.15K-323.15K. The temperature-dependent dielectric relaxation of the Gly/ NMP binary mixtures are determined by fitting the complex permittivity data in the frequency range 20 MHz-20 GHz by using Havriliak-Negami relation [58]. The chemicals chosen under study are based on scientific and practi-

cal importance in the field of pharmaceutical, medical and industrial research applications [33-41]. The motive behind the present study is to identify (i) molecular association between the liquid mixtures in terms of intermolecular hydrogen bonding (ii) assess the structural contribution in the system based on volumetric parameters (iii) effect of hydrogen bonding on dipole moment, relaxation behaviour and polarizability values (iv) infer the molecular polarizability of the Gly/NMP binary mixtures (v) compare the experimental dipole moment values with theoretical dipole moments which are obtained from DFT studies.

The novelty of the present work includes the understanding of nature of molecular interaction associated between solute and solvent molecules in terms of Helmholtz energy ( $\Delta F^E$ ) equation, calculation of dipole moments and bonding energy between Gly/NMP system using DFT methods with different basis sets. Further, analysed the effect of hydrogen bonding on relaxation behaviour of Gly/NMP binary mixture at different concentrations and temperatures apart from the regular thermophysical and excess dielectric parameters. In addition to this evaluated mean molecular polarizability calculations with different theoretical models and the presence of hydrogen bonding between the Gly, NMP is confirmed from the FT-IR spectra. The work output of the results might provide some useful information to large-scale pharmaceutical and industrial research applications.

## 2. Experimental

### 2.1. Materials

Analytical Reagent grade chemicals such as Glycerol (Gly), N-Methyl-2-Pyrrolidone (NMP) and benzene were procured from Sigma Aldrich India. These compounds further purified by double distillation procedure [59] and collected middle fractions of the chemical compound. These liquids are stored in dark bottles with molecular sieves (8Å) to prevent moisture absorption. The Gly/NMP binary mixtures are prepared for eleven-volume concentration ranges. Simultaneously weight measurements, mole fractions of the solute ( $x_1$ ) and solvent ( $x_2$ ) were also calculated. By using the specific gravity bottle method [60], the densities ( $\rho$ ) of pure as well as liquid binary mixtures are determined. The uncertainty in the mole fractions ( $x_1, x_2$ ) and the density ( $\rho$ ) measurement was estimated to be less than  $\pm 0.0001$ ,  $\pm 0.0001 \text{ kg m}^{-3}$ . The density ( $\rho$ ), low-frequency dielectric permittivity ( $\epsilon_0$  at 20 MHz), refractive index ( $n_D$ ), dipole moment ( $\mu$ ) and relaxation time ( $\tau$ ) values of pure liquids at 298.15K are listed in Table 1 and these values are compared with the reported literature values. The measured values are in good agreement with reported values within the error limits of 1-2%.

**Table 1**

Experimental and literature values for density ( $\rho$ ), refractive index ( $n_D$ ), dipole moment ( $\mu$ ), low-frequency dielectric permittivity ( $\epsilon_0$ ) and relaxation time ( $\tau$ ) of the pure liquids at 298.15K.

Liquid sample	Source/Purity	Density $\rho$ (g/cm <sup>3</sup> )		$\epsilon_0$ (20 MHz)		$n_D$		Dipole moment ( $\mu$ , D)		Relaxation time ( $\tau$ , ps)	
		This work	Literature <sup>†</sup>	This work	Literature	This work	Literature	This work	Literature	This work	Literature
Glycerol	Sigma-Aldrich/ 99%	1.2610	1.25791 [51]	42.45	41.17 [45] 42.50 [93] 43.0 [48] 42.70 [52]	1.4745	1.4729 [96] 1.48675 [97]	2.60	2.56 [52], †	1366	1400 [48]
			1.2614 [95]							1300 [52]	
NMP	Sigma-Aldrich/ 99.5%	1.0287	1.0285 [94]	32.38	32.60 [56] 32.0 [94]	1.4700	1.4701 <sup>†</sup>	4.14	4.10 <sup>†</sup> 4.30 [54]	21.12	20-25 [54]

Standard uncertainties  $u$  are  $u(\rho)=0.0002$ ,  $u(\epsilon_0)=2-3\%$ ,  $u(n_D)=0.0001$ ,  $u(\mu)=0.02\text{D}$  and  $u(\tau)=5-7\%$

<sup>†</sup> crc handbook of chemistry and physics (2003-2004), 84th edition, Pg No:6-157,6-162, CRC press

**Table 2**

The fitting parameters of Jouyban-Acree model [89] for density Vs. component concentration, and the average absolute deviations and degree of fitting for Gly/NMP system.

T/K	$\rho=f(x_1)$						R <sup>2</sup>
	a <sub>0</sub>	a <sub>1</sub>	a <sub>2</sub>	a <sub>3</sub>	a <sub>4</sub>	AAD%	
298.15	-10.6192	-1.0346	-0.0944	-0.0060	-0.0200	0.0000190	0.9934
303.15	-10.8437	-1.0507	-0.1100	-0.0123	-0.0015	-0.0000020	0.9934
308.15	-11.0754	-1.0699	-0.1119	-0.0125	-0.0015	-0.0000008	0.9934
313.15	-11.2843	-1.0883	-0.1138	-0.0127	-0.0016	0.0000020	0.9934
318.15	-11.5017	-1.1069	-0.1157	-0.0129	-0.0016	0.0000003	0.9934
323.15	-11.6738	-1.1240	-0.1175	-0.0131	-0.0016	-0.0000005	0.9934

## 2.2. Measurements

The experimental dipole moment ( $\mu$ ) of the pure liquids such as Gly and NMP and their equimolar binary mixtures are measured by using Higasi's method [61] in the temperature range i.e. 298.15K-323.15K. In order to determine the experiment dipole moments ( $\mu$ ) of pure liquids of Gly, NMP and their equimolar binary mixtures, dilute solutions of the pure liquids are prepared in non-polar solvent benzene in the concentration range of 0 to 1 ml in a 10 ml solution. The static dielectric constant ( $\varepsilon_s$ ) of these liquid samples are measured by using Dielectric constant measurement setup (Model DSL-01) supplied by SES Instrument Pvt. Ltd, Roorkee, India. Further, the optical refractive index ( $n_D$ ) is measured by Carl-Zeiss Abbe refractometer. The uncertainty in the measurement value of static dielectric constant and refractive indices are  $\pm 0.001$ ,  $\pm 0.0001$  units respectively. The dielectric permittivity ( $\varepsilon^* = \varepsilon' - j\varepsilon''$ ) of the binary liquid mixtures at different temperatures were measured in the microwave frequency range ( $0.02 < \nu/\text{GHz} < 20$ ) using open-ended high-performance coaxial probe kit (85070 E Keysight Technologies) and Vector Network Analyzer (Keysight E 8361C). We have measured the dielectric permittivity of the liquid samples only up to 20 GHz because coaxial cable supports only up to the frequency 20 GHz. There is an increase in the cable impedance losses and fluctuations in the spectra with a further increase in the frequency region leads to a high percentage of error in the measured data. The data obtained from the Vector Network Analyzer is analysed through lumped coaxial probe model [62–64]. To regulate the sample temperature, thermostat-controlled water circulation bath setup is used. The uncertainty involved in the measurement of temperature is about  $\pm 0.01\text{K}$ .

## 2.3. Determination of volumetric and dielectric parameters

Based on the volume fraction and density data at different temperatures i.e., 298.15K-323.15K, excess molar volume ( $V_m^E$ ), partial molar volume ( $V_{m,i}$ ), apparent molar volume ( $V_{\phi,i}$ ), coefficient of thermal expansion ( $\alpha_P$ ) [65–71] are evaluated and summarized in Table 3. The molar refraction ( $R_m$ ) [72], molar polarization ( $P_m$ ) [73,74] and excess refractive index ( $n_D^E$ ) [75] of the liquid binary system is obtained with the following mathematical expressions

$$R_m = \frac{(n_D^2 - 1)V_m}{(n_D^2 + 2)} \quad (1)$$

$$P_m = \frac{(\varepsilon - n_D^2)(2\varepsilon - n_D^2)V_m}{9\varepsilon} \quad (2)$$

$$n_D^E = n_D - (n_{D1}^2 x_1 + n_{D2}^2 x_2)^{1/2} \quad (3)$$

where  $\varepsilon$ ,  $n_D$  are the relative permittivity and refractive index,  $V_m$  is the molar volume of the mixture,  $P_m$  is the molar polarization,  $n_{D1}$ ,  $n_{D2}$ ,  $x_1$ ,  $x_2$  are the refractive index and molar fraction of the solute and solvent respectively.

In our previously published papers [76–78] and some of the dielectric literature [16–19,29,45,46] the evaluation of certain parameters such as excess dielectric field strength ( $\Delta\epsilon$ ), excess dipole moment ( $\Delta\mu$ ), excess dielectric permittivity ( $\varepsilon^E$ ), excess inverse relaxation time ( $1/\tau^E$ ), Kirkwood correlation factor ( $g^{eff}$ ) are explained. The excess volumetric and dielectric parameters such as  $V_m^E$ ,  $\varepsilon^E$ ,  $(1/\tau)^E$  were fitted with Redlich-Kister type polynomial equation [79] given as

$$y^E = x_1 x_2 \sum_{i=0}^4 A_i (x_1 - x_2)^i \quad (4)$$

where  $y^E$  indicates the excess values and  $A_i$  are the coefficients,  $x_1$  and  $x_2$  are the molar fractions of the solute and solvent. The standard deviation is obtained by using the below mathematical expression

$$\sigma = \left[ \frac{\sum (y_{exp}^E - y_{cal}^E)^2}{N - P} \right]^{0.5} \quad (5)$$

where  $N$  is the number of experimental points and  $P$  is the number of coefficients

The coefficients of Redlich-Kister polynomial equations  $A_0$ ,  $A_1$ ,  $A_2$ ,  $A_3$ ,  $A_4$ , and its standard deviation values are tabulated in Table 4.

From the temperature-dependent relaxation data, the thermodynamic quantities such as enthalpy of activation  $\Delta H^*$ , the entropy of activation  $\Delta S^*$  and Gibbs free energy of activation  $\Delta G^*$  are obtained from the following Eyring's rate equation [80,81].

$$\tau = \frac{h}{k_B T} e^{-\frac{\Delta G^*}{RT}} \quad (6)$$

where  $\Delta G^* = \Delta H^* - T \Delta S^*$ ,  $h$  is the Planck's constant,  $k_B$  is the Boltzmann constant and  $T$  is the temperature in Kelvin and  $R$  is the universal gas constant

The long-range and short-range interaction among the dipoles is determined from the excess Helmholtz energy ( $\Delta F^E$ ) equation [82] is given by

$$\Delta F^E = \Delta F_{or}^E + \Delta F_{rr}^E + \Delta F_{12}^E \quad (7)$$

where

$\Delta F_{or}^E$  = excess dipolar energy due to long-range electrostatic interaction

$\Delta F_{rr}^E$  = excess dipolar energy due to the short-range interaction between identical molecules

$\Delta F_{12}^E$  = excess free energy due to the short-range interaction between the dissimilar molecules

The mean molecular polarizability of Gly, NMP and their binary system is calculated by using the Lippincott  $\delta$ -function potential model [83,84] and these values are compared with the LeFevre method polarizability values [85]. To determine the mean molecular polarizability of Gly, NMP and their binary system, the optimized bond lengths data is used. These data obtained from density

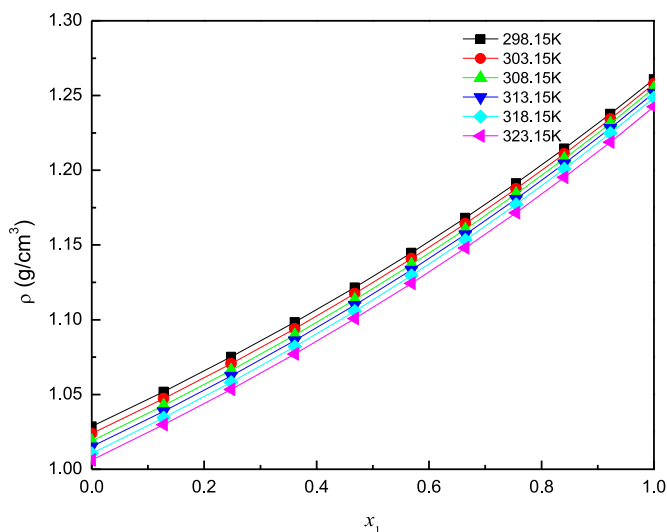


**Fig. 1.** Variation of density ( $\rho$ ) (fitted) values against the mole fraction ( $x_1$ ) of Gly in NMP medium at different temperatures.

functional theory (DFT-B3LYP) calculation method with 6-311G\*\* and cc-pVTZ basis sets. The presence of hydrogen bond between Gly and NMP is confirmed from the FT-IR spectra.

#### 2.4. Computational details

The optimised bond lengths of individual monomers of Gly, NMP and their dimer is determined from minimum energy geometry optimization procedure with DFT/B3LYP method using 6-311G\*\* and cc-pVTZ (correlation consistent-polarized valence triple zeta) basis sets [86–88] in a gaseous state. The single point energy is also evaluated for monomers and dimers to know the strength of hydrogen bond interactions between Gly and NMP molecules.

### 3. Results and discussion

The experimental density ( $\rho$ ) values of Gly/NMP and their binary mixtures of different compositions in the temperature range 298.15K–323.15K were represented in Fig. 1. From Fig. 1 it is noticed that experimental density ( $\rho$ ) values are increased with increase in Gly concentration in NMP solution and decreases with increase in temperature. The obtained values of density ( $\rho$ ) were fitted with Jouyban-Acree model [89] and the average deviations (AAD %) of densities are listed in Table 2. The measured experimental density values of Gly/NMP binary mixtures at various temperatures are listed in Table 3.

The calculated volumetric ( $V_m$ ) parameters such as excess molar volume ( $V_m^E$ ), partial molar volume ( $V_{m,i}$ ), apparent molar volume ( $V_{\varphi,i}$ ) and coefficient of thermal expansion ( $\alpha_p$ ) [65,66] of the binary mixtures are tabulated in Table 3. From Fig. 2, it is recognized that with an increase in Gly concentration in NMP medium, excess molar volume ( $V_m^E$ ) shows the negative value for all the temperatures and which suggests that decrease in the total molar volume of the composition compared with the simple linear summations. The decrease in volume is due to the presence of the hydrogen bond between components present in the mixture. Further,  $V_m^E$  values decrease with rising in temperature due to the decrease in the number of hydrogen bonds in the liquid system. The increase in thermal energy readily dissociates the number of hydrogen bond networks and reduces the charge transfer mechanism between components present in the liquid system. The volumetric, partial molar volume ( $V_{m,i}$ ) parameters facilitate to know the molecular interaction level between strongly polar substances and

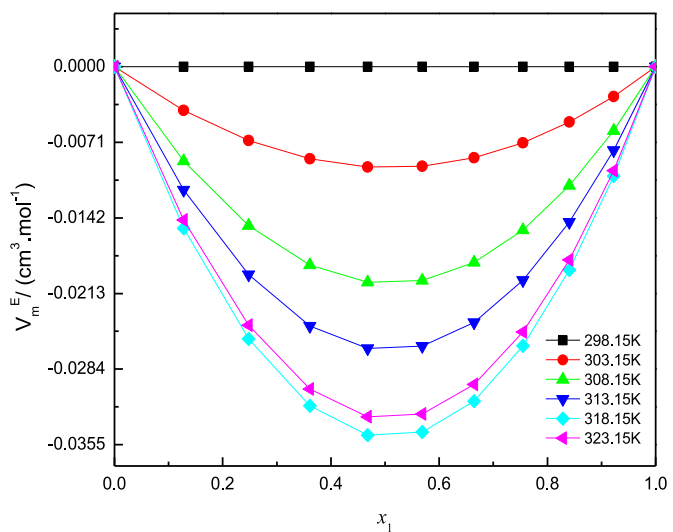


**Fig. 2.** Excess molar volume ( $V_m^E$ ) versus mole fraction ( $x_1$ ) of Gly in NMP medium at different temperatures.

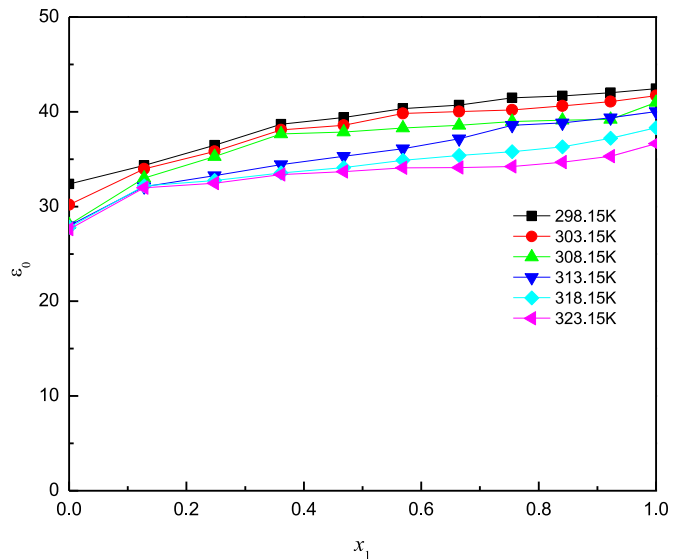


**Fig. 3.** Variation of low-frequency dielectric permittivity ( $\epsilon_0$ ) measured at 20 MHz versus mole fraction ( $x_1$ ) of Gly in NMP medium at different temperatures.

low-polar substance in the system. It also signifies the structural arrangement and the nature of the environment present in the liquid medium [65,90]. From Table 3 it is noted that the increase in  $V_{m,1}$  and  $V_{m,2}$  values with increase in temperatures indicates the change in the intermolecular forces present between Gly and NMP system.

The plot of dielectric permittivity ( $\epsilon_0$ ) measured at 20 MHz and high-frequency dielectric permittivity ( $\epsilon_\infty = n_D^{-2}$ ) at optical frequencies (Sodium light) against mole fraction of Gly in NMP medium as shown in Figs. 3 and 4 respectively. From Fig. 3 it is marked that the dielectric permittivity is increased with an increase in Gly concentration and it is due to the presence of hydrogen bond between Gly/NMP molecules. It also represents that molecular interaction changed from non-associative to self-associative nature. The higher dielectric permittivity values recommend that largely associated complexes are formed in the solution. From the Fig. 4 it is marked that the high-frequency dielectric permittivity ( $\epsilon_\infty$ ) value increased non linearly with increase in Gly concentration in NMP medium and which clearly represents the existence of heteromolecular in-

**Table 3**

Density ( $\rho$ ), excess molar volume  $V_m^E$ , partial molar volume  $V_{m,1}$ ,  $V_{m,2}$ , apparent molar volume  $V_{\phi,1}$ ,  $V_{\phi,2}$  and coefficient of thermal expansion ( $\alpha_p$ ) for the binary mixtures of Gly/NMP at different temperatures 298.15 K–323.15 K.

$x_1$	$\rho/\text{g cm}^{-3}$	$V_m^E/\text{cm}^3 \text{ mol}^{-1}$	$V_{m,1}/\text{cm}^3 \text{ mol}^{-1}$	$V_{m,2}/\text{cm}^3 \text{ mol}^{-1}$	$V_{\phi,1}/\text{cm}^3 \text{ mol}^{-1}$	$V_{\phi,2}/\text{cm}^3 \text{ mol}^{-1}$	$\alpha_p \times 10^4/\text{K}^{-1}$
<b>298.15K</b>							
0.00000	1.0287	0.0000	73.029	96.367	—	96.367	8.67
0.12787	1.0519	0.0000	73.029	96.367	73.029	96.367	8.30
0.24806	1.0752	0.0000	73.029	96.367	73.029	96.367	7.94
0.36124	1.0984	0.0000	73.029	96.367	73.029	96.367	7.61
0.46800	1.1216	0.0000	73.029	96.367	73.029	96.367	7.28
0.56889	1.1449	0.0000	73.029	96.367	73.029	96.367	6.97
0.66436	1.1681	0.0000	73.029	96.367	73.029	96.367	6.68
0.75484	1.1913	0.0000	73.029	96.367	73.029	96.367	6.39
0.84072	1.2145	0.0000	73.029	96.367	73.029	96.367	6.12
0.92234	1.2378	0.0000	73.029	96.367	73.029	96.367	5.85
1.00000	1.2610	0.0000	73.029	96.367	73.029	—	5.60
<b>303.15K</b>							
0.00000	1.0239	0.0000	73.176	96.824	—	96.824	8.71
0.12787	1.0472	-0.0041	73.186	96.823	73.183	96.819	8.33
0.24806	1.0706	-0.0069	73.194	96.822	73.187	96.815	7.98
0.36124	1.0940	-0.0087	73.200	96.819	73.191	96.810	7.64
0.46800	1.1174	-0.0094	73.205	96.815	73.195	96.806	7.31
0.56889	1.1408	-0.0093	73.208	96.811	73.199	96.802	7.00
0.66436	1.1642	-0.0086	73.211	96.807	73.202	96.798	6.70
0.75484	1.1876	-0.0071	73.213	96.802	73.206	96.795	6.41
0.84072	1.2110	-0.0052	73.214	96.797	73.209	96.791	6.13
0.92234	1.2344	-0.0028	73.215	96.792	73.212	96.788	5.87
1.00000	1.2578	0.0000	73.215	96.787	73.215	—	5.61
<b>308.15K</b>							
0.00000	1.0190	0.0000	73.300	97.285	—	97.285	8.75
0.12787	1.0426	-0.0089	73.322	97.284	73.315	97.274	8.37
0.24806	1.0662	-0.0149	73.339	97.280	73.324	97.265	8.01
0.36124	1.0898	-0.0186	73.352	97.274	73.333	97.255	7.67
0.46800	1.1134	-0.0202	73.362	97.266	73.341	97.247	7.34
0.56889	1.1370	-0.0201	73.370	97.257	73.349	97.238	7.02
0.66436	1.1605	-0.0184	73.375	97.248	73.357	97.230	6.72
0.75484	1.1841	-0.0153	73.379	97.238	73.364	97.222	6.43
0.84072	1.2077	-0.0112	73.382	97.227	73.371	97.214	6.15
0.92234	1.2313	-0.0060	73.384	97.217	73.378	97.207	5.88
1.00000	1.2549	0.0000	73.384	97.206	73.384	—	5.62
<b>313.15K</b>							
0.00000	1.0151	0.0000	73.456	97.658	—	97.658	8.78
0.12787	1.0388	-0.0116	73.484	97.657	73.475	97.645	8.40
0.24806	1.0624	-0.0195	73.507	97.652	73.487	97.632	8.04
0.36124	1.0861	-0.0243	73.524	97.644	73.499	97.620	7.69
0.46800	1.1098	-0.0265	73.537	97.634	73.510	97.609	7.36
0.56889	1.1335	-0.0262	73.547	97.623	73.520	97.597	7.04
0.66436	1.1571	-0.0240	73.554	97.610	73.530	97.587	6.74
0.75484	1.1808	-0.0201	73.559	97.597	73.540	97.577	6.45
0.84072	1.2045	-0.0146	73.563	97.583	73.549	97.567	6.17
0.92234	1.2281	-0.0079	73.565	97.569	73.558	97.557	5.90
1.00000	1.2518	0.0000	73.566	97.555	73.566	—	5.64
<b>318.15K</b>							
0.00000	1.0107	0.0000	73.617	98.088	—	98.088	8.82
0.12787	1.0344	-0.0152	73.654	98.087	73.642	98.071	8.44
0.24806	1.0582	-0.0256	73.683	98.080	73.657	98.054	8.07
0.36124	1.0820	-0.0319	73.705	98.070	73.672	98.038	7.72
0.46800	1.1058	-0.0346	73.722	98.057	73.687	98.023	7.39
0.56889	1.1296	-0.0343	73.735	98.042	73.700	98.009	7.07
0.66436	1.1534	-0.0314	73.745	98.025	73.713	97.995	6.76
0.75484	1.1771	-0.0262	73.752	98.008	73.726	97.981	6.47
0.84072	1.2009	-0.0191	73.756	97.990	73.738	97.969	6.19
0.92234	1.2247	-0.0103	73.759	97.972	73.749	97.956	5.91
1.00000	1.2485	0.0000	73.761	97.954	73.761	—	5.65
<b>323.15K</b>							
0.00000	1.0062	0.0000	73.980	98.522	—	98.522	8.86
0.12787	1.0298	-0.0144	74.015	98.521	74.004	98.506	8.48
0.24806	1.0535	-0.0243	74.043	98.514	74.019	98.490	8.11
0.36124	1.0771	-0.0303	74.064	98.505	74.033	98.475	7.76
0.46800	1.1007	-0.0329	74.080	98.492	74.046	98.460	7.42
0.56889	1.1244	-0.0326	74.093	98.478	74.059	98.446	7.10
0.66436	1.1480	-0.0298	74.102	98.462	74.072	98.433	6.79
0.75484	1.1716	-0.0249	74.108	98.446	74.084	98.421	6.50
0.84072	1.1952	-0.0181	74.113	98.429	74.095	98.408	6.21
0.92234	1.2189	-0.0098	74.115	98.412	74.106	98.397	5.94
1.00000	1.2425	0.0000	74.117	98.394	74.117	—	5.68

Standard uncertainties  $u$  are  $u(\rho)=0.0002$ ,  $u(x_1)=0.0002$ ,  $u(V_{m1}, V_{m2}, V_{\phi1}, V_{\phi2})=0.001 \text{ cm}^3 \text{ mol}^{-1}$ .

**Table 4**  
Redlich–Kister coefficient and standard deviation values for Gly/NMP binary mixtures at different temperatures.

Function	Temp.(K)	$A_0$	$A_1$	$A_2$	$A_3$	$A_4$	$\sigma$
$V_m^E$	298.15	0.0000	0.0000	0.0000	0.0000	0.0000	0.0000
	303.15	-0.0379	0.0014	-0.0000	0.0000	-0.0000	1.175e-4
	308.15	-0.0815	0.0028	-0.0001	0.0000	-0.0000	0.001124
	313.15	-0.0107	0.0036	-0.0001	0.0000	-0.0000	0.000805
	318.15	-0.1393	0.0046	-0.0002	0.0000	-0.0000	0.000050
	323.15	-0.1324	0.0044	-0.0001	0.0000	-0.0000	2.65e-5
	298.15	9.8084	6.2663	4.8456	-12.0864	-20.3065	0.000264
	303.15	14.0786	10.0261	-9.0217	2.0370	11.3250	0.008350
	308.15	14.1184	20.5510	22.5655	2.0079	-43.9630	0.007082
	313.15	5.28210	4.52730	32.6775	11.8814	-27.2563	0.022108
$\epsilon^E$	318.15	5.57380	7.60590	0.78330	22.9675	19.4853	0.003331
	323.15	7.21870	11.8151	-2.54810	21.7690	17.3244	0.008702
	298.15	-0.0876	-0.0700	-0.0881	-0.1714	-0.1213	0.005889
	303.15	-0.0962	-0.0839	-0.0914	-0.1372	-0.0902	0.007412
	308.15	-0.0948	-0.0765	-0.0713	-0.1307	-0.1010	0.007806
	313.15	-0.0957	-0.0701	-0.0765	-0.1275	-0.0873	0.003610
$(1/\tau)^E$	318.15	-0.0982	-0.0836	-0.1149	-0.1090	-0.0327	0.007585
	323.15	-0.0929	-0.0777	-0.0825	-0.0152	0.0302	0.013771

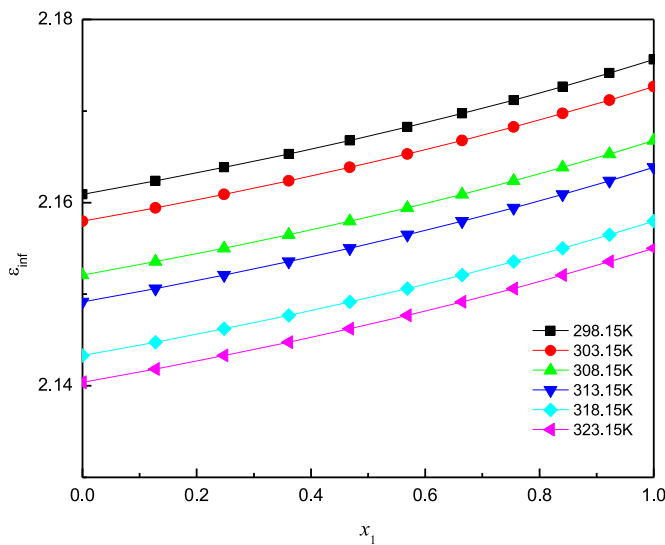


**Fig. 4.** The high-frequency dielectric constant ( $\epsilon_\infty = n_D^2$ ) versus mole fraction ( $x_1$ ) of Gly in NMP medium at different temperatures.

teraction in the binary liquid system. The heteromolecular interaction is occurred in the liquid due to the presence of electron donor-acceptor hydrogen bonding between Gly and NMP molecule. The variation of excess refractive index ( $n_D^E$ ) of Gly/NMP binary mixture is as shown in Fig. 5, and it noted that  $n_D^E$  values are negative at room temperature 298.15 K, and positive for remaining concentration ranges and other temperatures. In general, refractive indices indicate the propagation of light into the medium relative to the vacuum. For binary liquid mixtures,  $n_D$  depends not only on solute and solvent density but also on the parameters like intermolecular interaction, steric hindrance, the difference in molecular polarizability of the components and the temperature. The positive values of  $n_D^E$  represent the increase in charge-transfer complexes and intermolecular forces in the liquid mixture. The structural configuration about the chain length and molecular size differences in the liquid system can be obtained by molar polarization ( $P_m$ ) parameter. This parameter is derived from the Kirkwood–Frohlich equation [73,74] and it primarily depends on dielectric constant and dipole moment associated with the solute and solvent interactions. From Fig. 6, it is noticed that molar polarization ( $P_m$ ) value increased with the rise in Gly concentration in NMP medium and

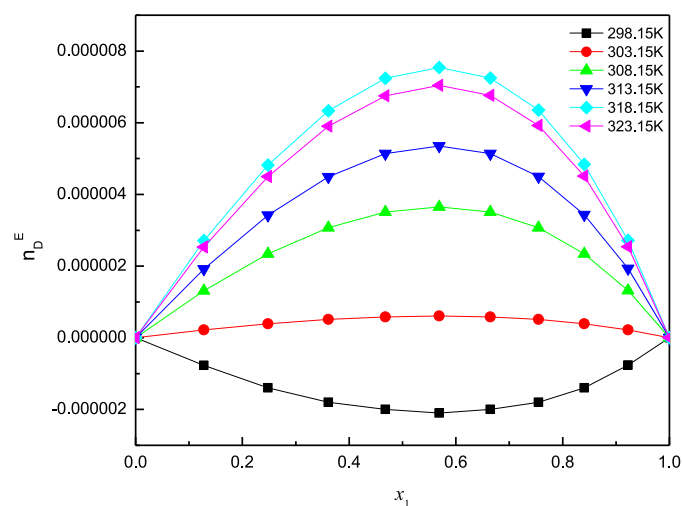


**Fig. 5.** Excess refractive index ( $n_D^E$ ) versus mole fraction ( $x_1$ ) of Gly in NMP medium at different temperatures.

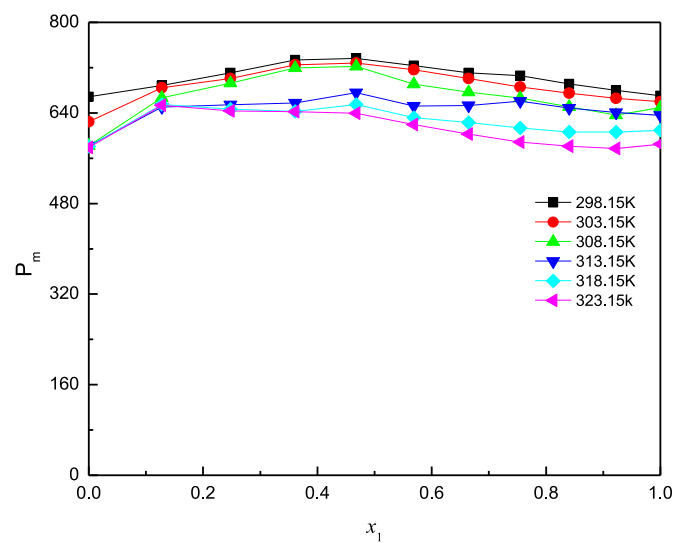


**Fig. 6.** Molar polarization ( $P_m$ ) against the mole fraction ( $x_1$ ) of Gly in NMP medium at different temperatures.

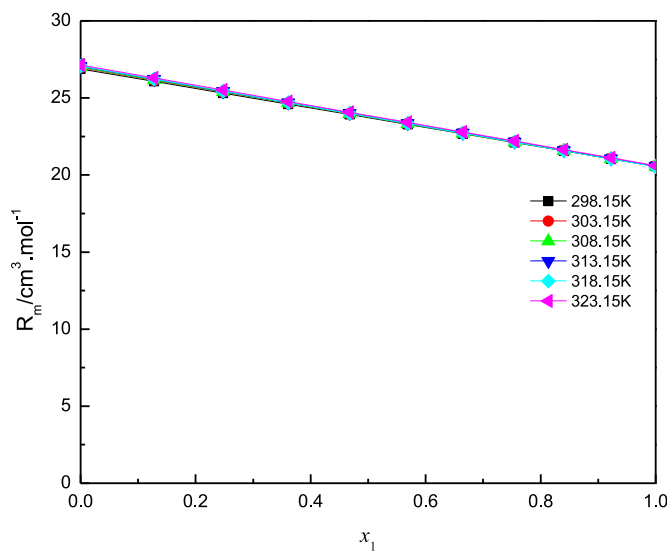


**Fig. 7.** Molar refraction ( $R_m$ ) against the mole fraction ( $x_1$ ) of Gly in NMP medium at different temperatures.

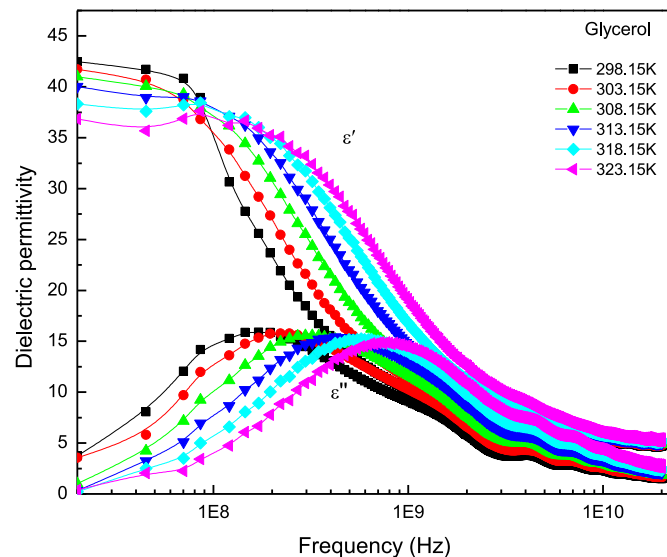


**Fig. 8.** Real ( $\epsilon'$ ) and imaginary part of dielectric permittivity ( $\epsilon''$ ) of Gly with respective frequency at different temperatures.

it shows the maximum value for the equimolar concentration of Gly/NMP binary mixture and thereafter decreases with increase in temperature. The maximum value of molar polarization ( $P_m$ ) is due to the presence of a strong hydrogen bond between Gly and NMP molecules and also the alignment of the dipoles in solution is highly favoured in the field direction. There is a decrease in the molar polarization value with a rise in temperature and it is due to a decrease in the dielectric susceptibility and randomization of electric dipoles in the solution. On the other hand, molar refraction ( $R_m$ ) value decreasing with the increase in Gly concentration and it is due to the increase in dispersion forces [72] as shown in Fig. 7. The high value of molar refraction of NMP indicates that more dipole-dipole interactions and low value of  $R_m$  represent self-associated or hydrogen bond interaction in Gly medium.

The real and imaginary part of the dielectric permittivity ( $\epsilon^* = \epsilon' - j\epsilon''$ ) of Gly, NMP and their equimolar binary mixtures at various temperatures as shown in Figs. 8, 9 and 10 respectively. From Figs. 8–10, it is observed that real part of the dielectric permittivity ( $\epsilon'$ ) value of Gly is higher when compared to NMP and

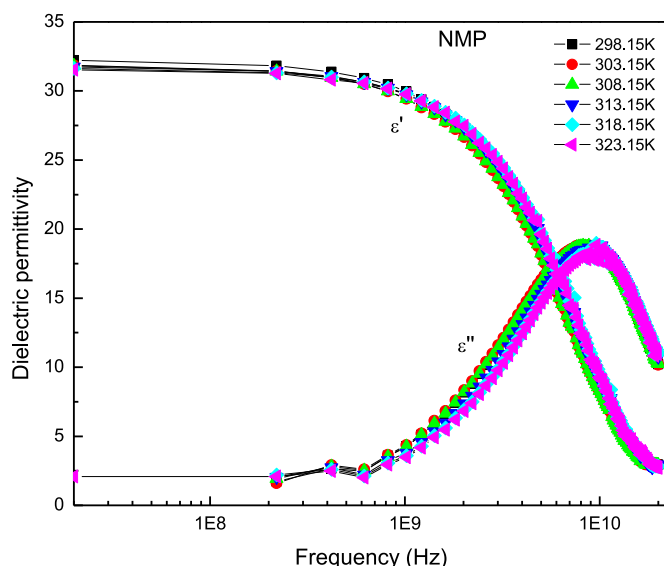


**Fig. 9.** Real ( $\epsilon'$ ) and imaginary part of dielectric permittivity ( $\epsilon''$ ) of NMP with respective frequency at different temperatures.

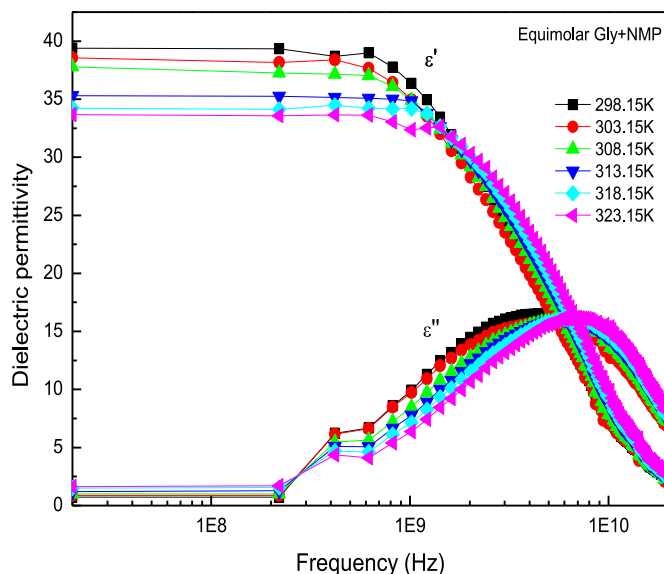


**Fig. 10.** Real ( $\epsilon'$ ) and imaginary part of dielectric permittivity ( $\epsilon''$ ) of equimolar binary mixtures of Gly/NMP with respective frequency at different temperatures.

other concentrations, and its value decreases with increase in frequency and temperature. The dielectric loss ( $\epsilon''$ ) is maximum for the equimolar concentration of Gly/NMP binary mixtures when compared to Gly, NMP and it is due to the presence of hydrogen bonds in the solution. Moreover, dielectric loss peak ( $\epsilon''$ ) of binary mixtures shifting towards higher frequencies with an increase in temperature and it might be due to fluctuations in the hydrogen-bonded network in the liquid system which is as shown in Fig. 10. Further, the width of the absorption peak ( $\epsilon''$ ) is wider when compared to the individual NMP (Fig. 9) and Gly (Fig. 8) liquids and it may be due to the presence of multimers in the solution. The dipole-dipole interaction between the NMP molecules causes the dielectric loss peak positioned at higher frequencies (GHz) for all the temperatures. Whereas for Gly (Fig. 8), dielectric loss peak is observed at lower frequencies (< 1 GHz) and it absorbs maximum electromagnetic energy due to self-associative nature phenomena. The self-associative nature of Gly is arisen due to formation of the intermolecular hydrogen bond between Gly-Gly molecules. The ab-

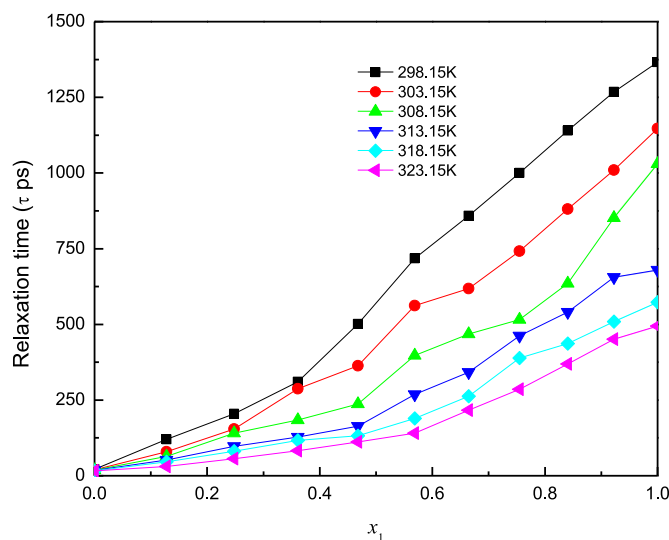


**Fig. 11.** Average relaxation time ( $\tau$ /ps) against mole fraction ( $x_1$ ) of Gly in NMP medium at different temperatures.

sorption peak of Gly is slightly shifting towards higher frequencies (0.145 GHz–0.471 GHz) with an increase in temperature and it may be due to disturbance in hydrogen bond networks in the solution.

Based on complex dielectric permittivity data ( $\epsilon^* = \epsilon' - j\epsilon''$ ), the average relaxation time ( $\tau$ ) of Gly/NMP binary mixtures are calculated using Havriliak-Negami relation [58] with the help of WINFIT software provided by NOVO Control Technologies as shown in Fig. 11. The Havriliak-Negami relation is used to fit the Cole-Davidson and Cole-Cole relaxation plots. The dielectric permittivity data of Gly is fitted with Cole-Davidson equation ( $\alpha=1$ ,  $0 < \beta < 1$ ) for all the temperatures. From curve fitting procedure using Havriliak-Negami relation, the shape factor ( $\beta$ ) of Gly is obtained and its value changes from 0.5350 to 0.5118 with the increase in temperature from 298.15K to 323.15 K. Whereas for NMP and remaining binary mixtures data is fitted with Cole-Cole equation and the value of  $\alpha$  is found to be in the range of  $0.9030 < \alpha < 1$ ,  $\beta=1$  for all the measured temperature ranges. The magnitude of the relaxation time value (See Fig. 11) of NMP is smaller (21.12ps) when compared to Gly (1366 ps) and other Gly/NMP concentrations. It is due to the non-associative nature of NMP molecules and the dipole-dipole interaction. The interaction energy between dipole-dipole is lesser when compared to hydrogen bond interaction. Further, with an increase in Gly concentration in NMP medium, it readily forms hydrogen bonding between -C=O group of NMP and hydroxyl group (-OH) of Gly and causes an increase in relaxation time values. There is an increase in the number of hydrogen bond networks in the solution which leads to the shift in dielectric absorption peak towards lower frequencies attributes higher relaxation time values. In the case of Gly, the relaxation time value (Fig. 11) is higher due to the presence of intermolecular hydrogen bonding between Gly molecules and also by its polyol nature. The increase in chain length between the molecules and steric hindrance property contributes to higher relaxation time value for Gly. The relaxation time value is decreased with increase in temperature and it is due to thermal energy dissociates the number of hydrogen bonds in the liquid system and further randomises the orientation of the dipoles in the field direction.

The molecular association between the binary liquid mixtures can be well interpreted by evaluating the excess parameters such as excess permittivity( $\epsilon^E$ ) and excess inverse relaxation time ( $1/\tau^E$ ) values. From Fig. 12, it is noted that the excess permittivity ( $\epsilon^E$ ) values are positive for all concentrations and temperatures of

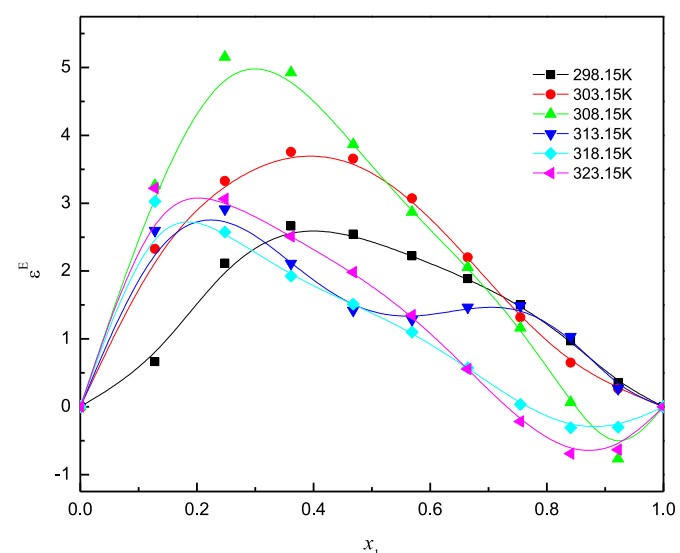


**Fig. 12.** Excess dielectric permittivity ( $\epsilon^E$ ) against mole fraction ( $x_1$ ) of Gly in NMP medium at different temperatures.

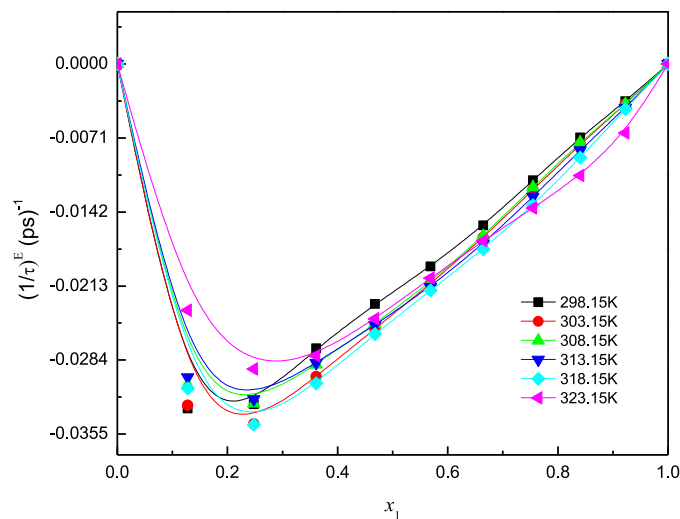


**Fig. 13.** Excess relaxation time ( $1/\tau^E$ ) against mole fraction ( $x_1$ ) of Gly in NMP medium at different temperatures.

Gly/NMP binary mixtures. Since the dielectric permittivity of both the molecules are additive, the positive behaviour of  $\epsilon^E$  represents the deviation from an ideal behaviour as a result of the presence of intermolecular association in Gly/NMP binary mixture. The molecular association in Gly /NMP binary mixture is due to the presence of hydrogen bond between the hydroxyl group (-OH) of Gly and -C=O group of NMP molecule. Further, the positive nature from an ideal behaviour represents that there is an increase in dipole moment per unit volume for Gly/NMP binary mixture which contribute the enhancement in dielectric polarization. For higher temperatures,  $\epsilon^E$  (Fig. 12) values are negative and which shows that the interaction between molecules in the mixture takes place in such a way that the effective dipole moment reduced and the distributions turn out to be more random. It suggests that there is a breakage of hydrogen bond networks in both Gly and NMP assembly. The different types of H- bond interactions and resultant dipolar association in the mixture may cause changes in the values of  $\epsilon^E$  at different temperatures. The plot of ( $1/\tau^E$ ) with the variation of mole fraction of Gly in NMP at various temperatures as shown in Fig. 13. From Fig. 13, it is noted that excess inverse relaxation

**Table 5**

Dipole moment ( $\mu$ ), temperature coefficient of the dipole moment  $d(\ln\mu^2)/dT$  and excess dipole moment ( $\Delta\mu$ ) of Gly, NMP and its equimolar binary mixture in the temperature range 298.15K-323.15K.

T (K)	Gly	NMP	Equimolar binary mixture (Gly + NMP)		$\Delta\mu = \mu_{AB} - (\mu_A + \mu_B)$ in D
	$\mu_A$ (D)	$10^3 d(\ln\mu^2)/dT$	$\mu_B$ (D)	$10^3 d(\ln\mu^2)/dT$	
298.15	2.60		4.14		5.78
303.15	2.58		4.12		5.76
308.15	2.57	-2.41	4.11	-1.73	5.73
313.15	2.55		4.09		5.70
318.15	2.54		4.07		5.69
323.15	2.52		4.05		5.67

Standard uncertainties u are  $u(\mu)=0.02D$  and  $u(T)=\pm 0.01K$

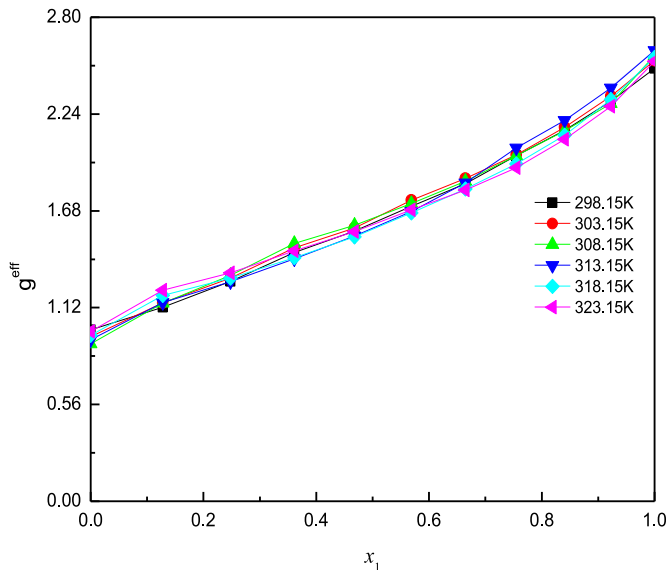


Fig. 14. Kirkwood effective ( $g_{eff}$ ) correlation factor versus mole fraction ( $x_1$ ) of Gly in NMP medium at different temperatures.

time values are negative [52,91] and it shows the existence of linear structures in the solution. These linear structures create a retarding field in the liquid medium in such a manner that effective dipoles rotate slowly in the liquid mixture.

The alignment of the dipoles and their molecular association is described by Kirkwood correlation  $g_{eff}$  factor. If  $g_{eff}$  factor  $< 1$  specifies the random orientation of the dipoles and  $g_{eff}$  factor  $> 1$  represents ordering nature of the dipoles. From Fig. 14, it is clear that  $g_{eff}$  factor increases with rise in Gly concentration in NMP medium and it is due to the interaction between the molecule's changes from non-associative to self-associative nature. The  $g_{eff}$  factor of NMP liquid is less than one which represents the lack of coordination among the NMP molecules due to lesser intermolecular energy. Whereas for Gly molecules, the high degree of polarization and cooperation among the dipoles causes  $g_{eff}$  factor value greater than one. The intermolecular hydrogen bonding between Gly molecules leads to greater polarization of the dipoles in the field direction. The nonlinear nature of  $g_{eff}$  plot represents the existence of hetero molecular interaction in the liquid mixture. Further,  $g_{eff}$  value decreases with an increase in temperature due to a decrease in the number of hydrogen bond networks in a liquid system. This corresponds to decrease in the cooperation among the dipoles and turns out the activated system into an unstable stable system.

The dipole moment ( $\mu$ ) of Gly, NMP and their equimolar binary mixture at different temperature 298.15K-323.15K are obtained from Higasi's method which is mentioned in Table 5. The determined dipole moments are compared with the available lit-

erature values and they are in good agreement with each other (Table 1). From Table 5, it is noticed that because of the solvent nature and presence of dipole-dipole interactions, the evaluated experimental dipole moments are slightly different from the literature values. Further, there is an increase in the experimental dipole moment value of equimolar binary system when compared to the pure Gly and NMP liquids. The increase in dipole moment is due to the presence of hydrogen bonding between Gly and NMP molecules. Further, the change in the dipole moment value may also depend upon the configuration, environment associated with the system. The dipole moments of the individual as well as equimolar binary system decreases with increase in temperature due to disturbance in the orientation of the dipoles. The temperature coefficient of the dipole moment  $d(\ln\mu^2)/dT$ , for Gly and NMP and their equimolar binary system, are also calculated and represented in Table 5. It is noticed that both the liquids exhibit a negative temperature coefficient of dipole moment values which differs in magnitude. The smaller in magnitude value of NMP indicates the molecular structure is less sensitive with vary in temperature and it is due to restriction involved in the movement of the molecule structure. Whereas the larger value of the temperature coefficient value of Gly suggests the more flexible structure of the molecule to form H-bonding with the nearby molecules (Self-association). The excess dipole moment ( $\Delta\mu$ ) provides the information related to the presence of ionic bonding or hydrogen bond exists between the components present in the liquid solution. The positive value of  $\Delta\mu$  represents the presence of ionic bond, the negative value of  $\Delta\mu$  indicates the presence of hydrogen bond in the liquid solution. From Table 5, it is noticed that  $\Delta\mu$  values are negative and which confirms the existence of H-bond or proton transfer in the bond.

The long-range and short-range interaction among the dipoles is evaluated by determining the excess Helmholtz energy ( $\Delta F^E$ ) equation in terms of the parameters  $\Delta F_{er}^E$ ,  $\Delta F_{rr}^E$ ,  $\Delta F_{12}^E$  which are tabulated in Table 6. The first term in the equation  $\Delta F_{er}^E$  describes the long-range interaction among the dipoles in the system. From Table 6, it is observed that most of the values of  $\Delta F_{er}^E$  are negative which describe there is an attractive force present between the dipoles in the system. The increase in temperature decreasing the strength of the interaction energy between Gly and NMP dipoles. Since the interaction energy depends on concentration, temperature and environment associated with the system. The second term  $\Delta F_{rr}^E$  reveals information about the short-range interaction among similar molecules. From Table 6 it is observed that the interaction energy is maximum with an increase in mole fraction of Gly in NMP medium. Further, the third term  $\Delta F_{12}^E$  indicates the strength of interactions between dissimilar molecules. The  $\Delta F_{12}^E$  values are negative which indicates the presence of heteromolecular interaction between the molecules and that readily forms the clusters in the solution. The volume occupied by the clusters in the solution depends upon the concentration and temperature. From Table 6, it is clear that most of the values of  $\Delta F^E$  are negative and which sug-

**Table 6**

Variation of  $\Delta F_{Or}^E$ ,  $\Delta F_{rr}^E$ ,  $\Delta F_{12}^E$  and  $\Delta F^E$  with the mole fraction of Gly in NMP medium at different temperatures.

$x_1$	$\Delta F_{Or}^E$ (J.mol $^{-1}$ )	$\Delta F_{rr}^E$ (J.mol $^{-1}$ )	$\Delta F_{12}^E$ (J.mol $^{-1}$ )	$\Delta F^E$ (J.mol $^{-1}$ )
<b>T=298.15K</b>				
0.00000	0.0000	0.0000	0.0000	0.0000
0.12787	-47.0268	-5.7575	1.7885	-50.9958
0.24806	-67.1335	-18.2738	1.9943	-83.4130
0.36124	-69.4956	-30.5523	-4.5728	-104.6207
0.46800	-49.3298	-27.7530	-9.8366	-86.9194
0.56889	-33.7873	-23.8652	-17.7025	-75.3549
0.66436	-17.5342	-14.6819	-21.4166	-53.6327
0.75484	-8.8760	-8.8678	-25.7684	-43.5122
0.84072	-0.3717	-0.4259	-22.2929	-23.0905
0.92234	2.4101	3.1675	-14.7009	-9.1233
1.00000	0.0000	0.0000	0.0000	0.0000
<b>T=303.15K</b>				
0.00000	0.0000	0.0000	0.0000	0.0000
0.12787	-99.4840	-14.6798	1.3411	-112.8227
0.24806	-101.4607	-29.4935	0.1000	-130.8542
0.36124	-95.5910	-44.4851	-9.2863	-149.3624
0.46800	-65.3763	-38.0060	-14.9695	-118.3518
0.56889	-46.6789	-34.6272	-26.6094	-107.9155
0.66436	-24.5275	-21.2846	-29.5918	-75.4039
0.75484	-8.1481	-8.1799	-29.5756	-45.9036
0.84072	0.9399	1.0941	-26.8949	-24.8608
0.92234	4.0364	5.4205	-18.0380	-8.5811
1.00000	0.0000	0.0000	0.0000	0.0000
<b>T=308.15K</b>				
0.00000	0.0000	0.0000	0.0000	0.0000
0.12787	-140.5647	-20.5114	0.9603	-160.1158
0.24806	-140.5473	-43.2196	-2.4293	-186.1963
0.36124	-125.8054	-61.7583	-15.4743	-203.0380
0.46800	-83.9003	-50.0520	-21.2711	-155.2234
0.56889	-52.1603	-37.6918	-28.1949	-118.0470
0.66436	-25.9880	-22.1194	-32.0109	-80.1182
0.75484	-7.8515	-7.8412	-33.8748	-49.5674
0.84072	6.5172	7.4482	-28.6818	-14.7164
0.92234	15.4082	20.0213	-17.7943	17.6352
1.00000	0.0000	0.0000	0.0000	0.0000
<b>T=313.15K</b>				
0.00000	0.0000	0.0000	0.0000	0.0000
0.12787	-120.1708	-17.9152	1.3437	-136.7423
0.24806	-106.6591	-28.8532	1.2613	-134.2510
0.36124	-85.8684	-34.5924	-2.4839	-122.9446
0.46800	-60.0901	-32.1535	-8.4938	-100.7374
0.56889	-36.2717	-24.5097	-15.8934	-76.6748
0.66436	-19.0432	-16.0214	-25.3845	-60.4492
0.75484	-10.6943	-11.1718	-36.0115	-57.8777
0.84072	1.0504	1.2633	-31.5515	-29.2378
0.92234	4.4631	6.2071	-21.2613	-10.5911
1.00000	0.0000	0.0000	0.0000	0.0000
<b>T=318.15K</b>				
0.00000	0.0000	0.0000	0.0000	0.0000
0.12787	-125.6054	-23.8638	0.8455	-148.6237
0.24806	-100.4300	-29.2780	0.6423	-129.0657
0.36124	-77.0802	-31.5583	-2.2119	-110.8504
0.46800	-51.8725	-27.4620	-6.5064	-85.8409
0.56889	-31.5375	-21.0939	-13.4422	-66.0736
0.66436	-12.5232	-10.1059	-18.4203	-41.0495
0.75484	2.6036	2.4773	-20.7615	-15.6806
0.84072	11.4123	12.7427	-20.5961	3.5589
0.92234	10.2007	13.5084	-16.3343	7.3749
1.00000	0.0000	0.0000	0.0000	0.0000
<b>T=323.15K</b>				
0.00000	0.0000	0.0000	0.0000	0.0000
0.12787	-125.9323	-27.7656	0.2208	-153.4771
0.24806	-99.6870	-32.0179	-0.8545	-132.5593
0.36124	-80.1376	-35.9947	-5.7702	-121.9025
0.46800	-53.2249	-29.8106	-9.6619	-92.6974
0.56889	-31.6142	-21.6686	-14.6113	-67.8942
0.66436	-10.5043	-8.4081	-15.6661	-34.5786
0.75484	5.3372	4.9618	-15.8287	-5.5297
0.84072	12.9824	14.1954	-16.3388	10.8390
0.92234	13.9329	17.8916	-12.6058	19.2186
1.00000	0.0000	0.0000	0.0000	0.0000

**Table 7**

Variation of thermodynamical parameters  $\Delta G^*$ ,  $\Delta H^*$ , and  $\Delta S^*$  with respective mole fraction of Gly/ NMP binary mixture at different temperatures.

$x_1$	T/K	$\Delta H^*/(\text{kJ}/\text{mole})$	$\Delta G^*/(\text{kJ}/\text{mole})$	$\Delta S^*/(\text{kJ}/\text{mole}/\text{K})$
0	298.15 (NMP)		12.08	-0.0214
	303.15	5.72	12.10	-0.0210
	313.15		12.28	-0.0213
	318.15		12.37	-0.0212
	323.15		12.42	-0.0211
	0.12787 298.15	32.03	12.61	-0.0213
	303.15		16.39	0.0685
	308.15	36.79	15.65	0.0698
			15.41	0.0694
			15.16	0.0691
			15.12	0.0681
			14.34	0.0695
	0.24806 298.15	41.52	17.72	0.0665
	303.15		17.33	0.0667
	308.15	37.53	17.44	0.0652
			16.79	0.0663
			16.62	0.0658
			15.93	0.0669
	0.36124 298.15	41.52	18.74	0.0764
	303.15		18.90	0.0746
	308.15		18.12	0.0760
			17.51	0.0767
			17.59	0.0752
			16.99	0.0759
	0.46800 298.15		19.93	0.0921
	303.15		19.49	0.0920
	308.15	47.38	18.77	0.0929
			18.15	0.0934
			17.91	0.0927
			17.79	0.0916
	0.56889 298.15		20.82	0.1024
	303.15		20.60	0.1014
	308.15	51.32	20.09	0.1014
			19.44	0.1019
			18.86	0.1021
			18.41	0.1019
	0.66436 298.15		21.27	0.0699
	303.15		20.83	0.0702
	308.15	42.09	20.51	0.0701
			20.07	0.0704
			19.73	0.0703
			19.57	0.0697
	0.75484 298.15		21.64	0.0464
	303.15		21.30	0.0468
	308.15	35.47	20.76	0.0478
			20.85	0.0467
			20.77	0.0462
	0.84072 298.15		21.97	0.0392
	303.15		21.73	0.0393
	308.15	33.64	21.29	0.0401
			21.26	0.0395
			21.08	0.0395
			21.00	0.0391
	0.92234 298.15		22.23	0.0316
	303.15		22.07	0.0316
	308.15	31.66	22.04	0.0312
			21.76	0.0316
			21.48	0.0320
			21.54	0.0313
1	298.15 (Gly)		22.42	0.0322
	303.15	32.03	22.39	0.0318
			22.53	0.0308
			21.86	0.0325
			21.79	0.0322
			21.79	0.0317

**Table 8**

Experimental, theoretical dipole moments ( $\mu$ ) and mean molecular polarizability ( $\alpha_M$ ) of Gly, NMP and their equimolar binary systems at 298.15K.

Dipole moment in Debye System/Basis sets	Gaseous state DFT/B3LYP 6-311G** cc-pVTZ	Experiment Higasis's method	Polarizability ( $\alpha_M$ ) $\times 10^{-25}$ cm $^3$ Lippincott- $\delta$ function	LeFevre method
Glycerol (Gly)	2.21D	3.26D	88.937	80.69
Energy (a.u), $E_{\text{Gly}}$	-343.876	-344.920		
NMP	4.59D	4.11D	4.14D	112.246
Energy (a.u), $E_{\text{NMP}}$	-325.933	-325.985		106.26
Equimolar binary mixtures (Gly+NMP)	6.68D	6.72 D	5.78D	206.530
Energy (a.u) $E_{\text{Gly+NMP}}$	-669.832	-670.938		193.75
The difference in energy (kcal/mole) $E_T = E_{\text{Gly+NMP}} - (E_{\text{Gly}} + E_{\text{NMP}})$	14.43	16.31		

Uncertainties u in  $u(\mu)=0.02\text{D}$  and  $u(E)=0.0002$

In 6-311G \*\*, asterisks indicate the polarization functions d, p is added to 6-311G basis set

cc-pVTZ indicates correlation consistent-polarized valence triple zeta basis set

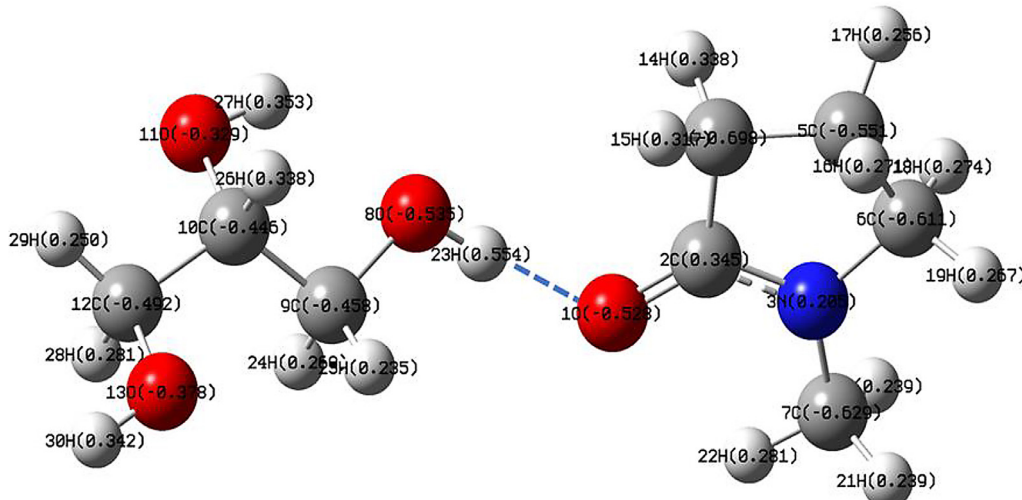


**Fig. 15.** Optimized converged geometrical structure of the hydrogen-bonded system of Gly/ NMP in the gaseous state from DFT 6-311G\*\* basis set using Gaussian-09 (with full natural bond analysis (NBO)).

gests the presence of  $\alpha$ - clusters in the solution. For higher temperatures and mole fractions (0.8 to 1, > 308.15K),  $\Delta F^E$  values are positive which describes the existence of  $\beta$ -clusters in the solution. The presence of  $\alpha$ -clusters in the solution enhances the effective dipole moment of the binary system and which in turn increases the internal energy of the system.

From the Eyring's rate equations [80,81], thermodynamic parameters such as enthalpy of activation  $\Delta H^*$ , entropy of activation  $\Delta S^*$  and Gibbs free energy of activation  $\Delta G^*$  are determined and listed in Table 7. The heat energy is taken in or given out in the reaction is known as bond dissociation energy. If the heat energy is obtained from the surrounding then it is called endothermic or if the heat is given out to the surroundings then it is said to be the exothermic reaction. Therefore  $\Delta H^*$  vale is positive for endothermic reaction and negative for an exothermic reaction. From Table 7, it is seen that  $\Delta H^*$  values are positive and increases up to equimolar concentration and thereafter decreases with increase in Gly concentration. It is due to the interaction between the molecule's changes from dipole-dipole (NMP-NMP) to hydrogen bonding (Gly-Gly) interaction. The positive values of  $\Delta H^*$  evidence that the environment of the system is in favour of hydrogen bond formation in the liquid mixture. The Gibbs free energy of activation  $\Delta G^*$  represents the strength of the interaction between unlike molecules in the solution. From Table 7, it is seen that  $\Delta G^*$  value increases with increase in Gly concentration in NMP medium due to the interaction between the molecule's changes from non-associative to self-associative nature. The interaction energy is maximum for higher concentration of Gly when compared to NMP and decreases

with rising in temperature. The entropy of activation  $\Delta S^*$  suggests the clue about the orientation process of the dipoles and also activated status of the system. Further, the positive value of  $\Delta S^*$  indicates the transition state with looser bonds or dissociative mechanism in the system. Whereas negative values of  $\Delta S^*$  represents a more ordered unimolecular process or associative mechanism in which two reaction partners form a single activated complex in the system [92]. For all the concentrations and temperatures except pure NMP system, the  $\Delta S^*$  values are positive which indicates that the environment of the system is restricting the alignment of the dipoles in the field direction.

The theoretical dipole moment, single-point energy calculations of individual monomers of Gly, NMP and their dimer is evaluated by using DFT/B3LYP method with 6-311G\*\* and cc-pVTZ basis sets and molecular polarizability values which are summarized in Table 8. The bond lengths obtained from the minimum energy geometry optimization procedure are used to evaluate the mean molecular polarizability of the components using Lippincott  $\delta$ -function potential model [83,84]. These polarizability values are compared with the LeFevre method [85] of polarizability values. From Table 8, it noticed that there is little variation in experimental dipole moment values when compared to the theoretical dipole moment values. It is due to  $\pi$ - electron cloud of non-polar solvent benzene influencing the solute dipole moment properties. The mean molecular polarizability of the Gly/NMP binary mixture is greater when compared to Gly and NMP system and it is due to the presence of hydrogen bonding between Gly and NMP molecules. The mean molecular polarizability value calculated from

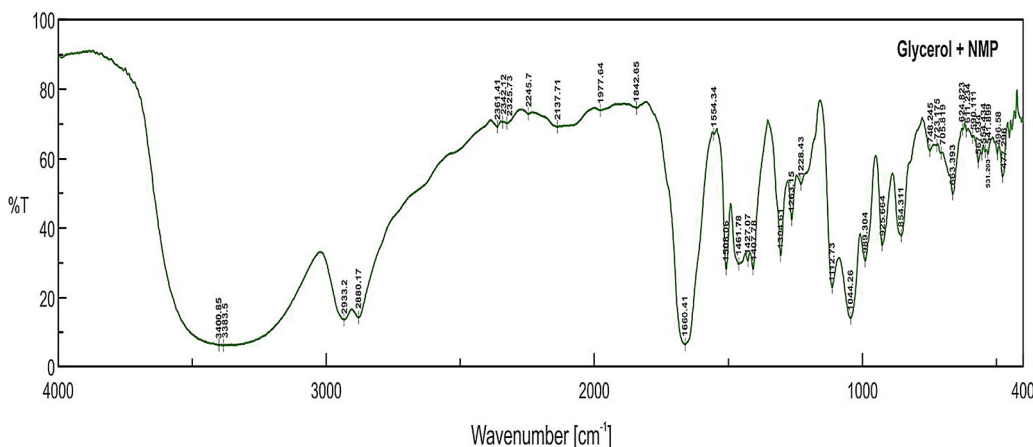


**Fig. 16.** FT-IR spectra of an equimolar concentration of Gly and NMP liquid.

both of the methods are in good agreement with each other. The difference in interaction energy associated between Gly and NMP molecules lies between 14–16 kcal/mole (See Table 8). This interaction energy confirms the presence of the hydrogen bond between Gly and NMP molecules. From the Natural Bond Orbital (NBO) analysis and minimum energy geometry optimization procedure, one of the possible combinations of Gly/NMP conformer structure and the location of hydrogen bonding as shown in Fig. 15. The dipole moment obtained with these conformer structures nearly shows similar value to that of experimental dipole moment values when compared to other possible combinations. The obtained results support the presence of hydrogen bonding between Gly / NMP molecules in the liquid system.

From the FT-IR spectrum of Gly and NMP liquids, it is noticed that there is a strong vibrational stretching at  $3474\text{ cm}^{-1}$  and  $1680\text{ cm}^{-1}$  for -OH and -C=O groups. After observing the FTIR spectra of equimolar binary mixtures of Gly and NMP which is as shown in Fig. 16, the stretching frequencies of -OH and -C=O decreased to  $3400\text{ cm}^{-1}$  and  $1660\text{ cm}^{-1}$  respectively. The decrease in wavenumbers is due to the presence of strong interaction between the -OH of Gly and -C=O group of NMP (See Fig. 15). Therefore FT-IR spectrum supports the existence of intermolecular hydrogen bonding between Gly and NMP liquid system.

#### 4. Conclusions

The concentration-dependent dielectric relaxation behaviour of Gly/ NMP binary mixtures at microwave frequency region (20 MHz–20 GHz) have been investigated in the temperature range 298.15K–323.15K. The relaxation spectra can well be interpreted by Cole–Davidson and Cole–Cole model plots. The relaxation time value is increased with an increase in Gly concentration in NMP medium due to interaction between the molecules changed from non-associative to self-associate nature. The self-associated nature of Gly molecules leads to the high degree of susceptibility and orientation polarizability values. The negative values of excess molar volume ( $V_m^E$ ) for entire concentrations and temperature range suggests the existence of strong hydrogen bonding in the liquid system. The presence of hydrogen bonding between Gly and NMP is strongly supported by the changes in the values of dielectric relaxation, effective dipole moment, excess Helmholtz energy ( $\Delta F^E$ ) and thermodynamic parameters. The mean molecular polarizability value calculated from Lippincott  $\delta$ -function potential model are in good agreement with the LeFevre method of polarization values. The computed dipole moment values using DFT/B3LYP method with 6-311G\*\* and cc-pVTZ basis sets are also in accordance with the experimental values. The FT-IR spectra evidences the exis-

tence of inter molecular hydrogen bonding between Gly and NMP molecules in the liquid system.

#### Declaration of Competing Interest

The authors declare that they have no known competing financial interests or personal relationships that could have appeared to influence the work reported in this paper.

#### Acknowledgements

The authors gratefully acknowledge University Grants Commission Networking Resource Centre, School of Physics, [University of Hyderabad](#), for giving the opportunity to use their Research lab facilities to carry out the above work.

#### Supplementary materials

Supplementary material associated with this article can be found, in the online version, at [doi:10.1016/j.molstruc.2020.129703](https://doi.org/10.1016/j.molstruc.2020.129703).

#### References

- [1] U. Kaatze, Meas. Sci. Technol. 19 (2008) 1–4 112001.
- [2] J.P.M Jiménez, J.M.F. Marquina, D. Dígon Rodríguez, S. Otín Lacarra, J. Mol. Liq. 139 (2008) 48–54.
- [3] R. Buchner, Pure Appl. Chem. 6 (2008) 1239–1252.
- [4] A.M. Navarro, B. García, S. Ibeas, F.J. Hoyuelos, I.A. Peñacoba, JM. Leal, J. Phys. Chem. B 117 (39) (2013) 11765–11771.
- [5] P.M Kumar, M. Malathi, J. Mol. Liq. 145 (2009) 5–7.
- [6] Y. Yomogida, Y. Sato, R. Nozaki, T. Mishina, J. Nakahara, J. Mol. Liq. 154 (2010) 31–35.
- [7] A. Mohan, M. Malathi, A.C. Kumbharkhane, J. Mol. Liq. 222 (2016) 640–647.
- [8] R.J. Sengwa, P. Dhatarwal, S. Choudhary, J. Mol. Liq. 271 (2018) 128–135.
- [9] K.B. Kabara, K. H.Wanjanje, A. C.Kumbharkhane, AV. Sarode, J. Mol. Liq. 299 (2020) 112137.
- [10] P.P. Kannan, N.K. Karthick, A. Mahendraprabu, A.C. Kumbharkhane, G. Arivazhagan, J. Mol. Struct. 1183 (2019) 60–69.
- [11] J. Preto, M. Pettini, J.A. Tuszyński, Phys. Rev. E 91 (2015) 052710.
- [12] R.M. Shirke, A. Chaudhari, N.M. More, P.B. Patil, J. Chem. Eng. Data. 45 (5) (2000) 917–919.
- [13] K. Dharmalingam, K. Ramachandran, P. Sivagurunathan, G.M. Kalamse, J. Chem. Eng. Data. 52 (1) (2006) 265–269.
- [14] M. Moghadam, T. Ghorbanpour, J. Chem. Thermodyn. 113 (2017) 263–275.
- [15] L.S. Gabrielyan, S.A. Markarian, J. Mol. Liq. 162 (2011) 135–140.
- [16] B.G. Lone, P.B. Undre, S.S. Patil, P.W. Khirade, S.C. Mehrotra, J. Mol. Liq. 141 (2008) 47–53.
- [17] K. Klimaszewski, A. Bald, R.J. Sengwa, S. Choudhary, Phys.Chem.Liq. 51 (2013) 532–546.
- [18] Y. Yomogida, Y. Sato, K. Yamakawa, R. Nozaki, J. Nakahara, J. Mol. Struct. 970 (2010) 171–176.
- [19] B. Lone, V. Madhurima, J. Mol. Model. 17 (2011) 709–719.
- [20] S. Schrödle, G. Heftet, R. Buchner, J. Phys. Chem. B 111 (2007) 5946–5955.
- [21] T. Yamaguchi, H. Furuhashi, T. Matsuoka, S. Koda, J. Phys. Chem. B 112 (2008) 16633–16641.

- [22] P.B. Undre, P.W. Khirade, V.S. Rajenimbalkar, S.N. Helambe, S.C. Mehrotra, *Phys Chem Liq* 50 (2012) 637–651.
- [23] E.H. Grant, R.J. Sheppard, G.P. South, *Dielectric Behaviour of Biological Molecules in Solutions*, Clarendon Press, Oxford, 1978.
- [24] V'a Raicu, Y. Feldman, *Dielectric Relaxation in Biological Systems-Physical Principles, Methods, and Applications*, Oxford University Press, United Kingdom, 2015.
- [25] A. Shahzad, S. Khan, M. Jones, R.M. Dwyer, M. O'Halloran, *Biomed. Phys. Eng. Express* 3 (2017) 045001.
- [26] CD. Abeyrathne, MN. Halgamuge, PM. Farrell, E. Skafidas, *Sci. Rep.* 3 (1796) 1–5 2013.
- [27] V. Choudhary, B.P. Singh, *Polymer Nanocomposites for Electromagnetic Interference Shielding*, Elsevier, 2018.
- [28] S. Gabriel, R.W. Lau, C. Gabriel, *Phys. Med. Biol.* 41 (11) (1996) 2271–2293.
- [29] T.A. Taha, N. Hendawy, S. El-Rabaie, A. Esmat, M.K. El-Mansy, *J. Mol. Struct.* 1212 (2020) 128162.
- [30] T.A. Taha, S.A. Saad, *Mater. Chem. Phys.* 255 (2020) 123574.
- [31] T.A. Taha, A. Hassona, S. Elrabaie, M.T. Attia, *Appl.Phys. A* 126 (2020) 1–10.
- [32] T.A. Taha, M.M. El-Molla, *J. Mater. Res. Technol.* 9 (2020) 7955–7960.
- [33] T.A. Taha, A.A. Azab, E.H. El-Khawas, *J. Electron. Mater.* 49 (2020) 1161–1166.
- [34] B. Katryniok, S. Paul, V. Bellière-Baca, P. Reye, F. Dumeignil, *Green Chem.* 12 (2010) 2079–2098.
- [35] R. Christoph, B. Schmidt, U. Steinberger, W. Dilla, R. Karinen, *Ullmann's Encyclopedia of Industrial Chemistry*, 2000.
- [36] A. Farrán, C. Cai, M. Sandoval, Y. Xu, J. Liu, M.J. Hernández, R.J. Linhardt, *Chem. Rev.* 115 (2015) 6811–6853.
- [37] JL García, H. García-Marín, E. Pires, *Green Chem.* 16 (2014) 1007–1033.
- [38] M. Gurgel Adeodato Vieira, M.A. Silva, L.O. Santos, M.M. Beppu, *Eur. Polym. J.* 47 (2011) 254–263.
- [39] EI. Stout, A. McKesson, *Adv. Wound Care* 1 (2012) 48–51.
- [40] A. Jouyban, M.A.A. Fakhree, A. Shayanfar, *J. Pharm. Pharm. Sci.* 13 (2010) 524–535.
- [41] M. Roche-Molina, B. Hardwick, C. Sanchez-Ramos, D. Sanz-Rosa, D. Gewert, FM. Cruz, A. Gonzalez-Guerra, V. Andres, JA. Palma, B. Ibanez, G. McKenzie, JA. Berna, *Sci. Rep.* 10 (2020) 11636.
- [42] N. Menon, K.P. O'Brien, PK. Dixon, L. Wu, SR. Nagel, BD. Williams, J.P. Carini, *J. Non-Cryst. Solids* 141 (1992) 61–65.
- [43] Y. Hayashi, A. Puzenko, Y. Feldman, *J. Non-Cryst. Solids* 352 (2006) 4696–4703.
- [44] M. Kohler, P. Lunkenheimer, A. Loidl, *Euro. Phys. J. E* 27 (115) (2008) 1–8.
- [45] R.J. Sengwa, S. Sankhla, V. Khatri, *Fluid Phase Equilib.* 285 (2009) 50–53.
- [46] R.J. Sengwa, V. Khatri, S. Choudhary, S. Sankhla, *J. Mol. Liq.* 154 (2010) 117–123.
- [47] A.A. Pronin, K. Trachenko, M.V. Kondrin, A.G. Lyapin, V.V. Brazhkin, *Phys. Rev. B* 84 (2011) 012201.
- [48] U. Kaatze, *Chem.Phys.* 403 (2012) 74–80.
- [49] R. Behrends, K. Fuchs, U. Kaatze, Y. Hayashi, Y. Feldman, *J. Chem. Phys.* 124 (2006) 144512.
- [50] A. Puzenko, Y. Hayashi, YE. Ryabov, I. Balin, Y. Feldman, U. Kaatze, R. Behrends, *J. Phys. Chem. B* 109 (2005) 6031–6035.
- [51] GI. Egorov, DM. Makarov, AM. Kolker, *Thermochim. Acta* 570 (2013) 16–26.
- [52] G.-Z. Jia, Q. Jie, W. Feng, *J. Mol.Struct.* 1100 (2015) 354–358.
- [53] Y. Chabouni, F. Amireche, *J. Chem. Eng. Data* 65 (4) (2020) 1679–1694.
- [54] G.-Z. Jia, W. Feng, Q. Jie, *J. Mol. Liq.* 197 (2014) 328–333.
- [55] A. Zaichikov, *Russ. J.Gen.Chem.* 76 (2006) 626–633.
- [56] H. Peter Bennetto Geoffrey, F. Evans, RJ. Sheppard, *J. Chem. Soc., Faraday Trans. 1* (79) (1983) 245–251.
- [57] J.-C. Liu, G.-Z. Jia, S. Liu, *Colloid. Polym. Sci.* 293 (2015) 289–296.
- [58] S. Havriliak, S. Negami, *Polymer* 8 (1967) 161–210.
- [59] D.D. Perrin, W.L.F. Armarego, *Purification of Lab Chem*, third ed., Pergamon Press, Oxford, 1980.
- [60] S.S. Sastry, B. Shaik, T. Vishwam, S.T. Ha, *Phys. Chem. Liq.* 52 (2) (2014) 272–286.
- [61] R. Minami, K. Itoh, H. H. Takahashi, K. Higasi, *J. Chem. Phys.* 73 (1980) 3396–3397.
- [62] U. Kaatze, *Metrologia* 47 (2010) S91–S113.
- [63] F. Kremer, A. Schonhals, *Broadband Dielectric Spectroscopy*, Springer, Berlin, 2003.
- [64] Y.Z. Wei, S. Sridhar, *Rev. Sci. Instrum.* 60 (1989) 3041–3046.
- [65] L. Mohammadi, A. Omrani, *J. Therm. Anal. Calorim.* 131 (2018) 1527–1543.
- [66] L. Mohammadi, A. Omrani, *J. Mol. Liq.* 241 (2017) 163–172.
- [67] AM. Awwad, AH. Al-Dujaili, HE. Salman, *J. Chem. Eng. Data* 47 (3) (2002) 421–424.
- [68] X. Yue, L. Zhao, L. Ma, H. Shi, T. Yang, J. Zhang, *J. Mol. Liq.* 263 (2018) 40–48.
- [69] WE. Acree Jr, F. Martínez, *J. Mol. Liq.* 272 (2018) 237–238.
- [70] H. Iloukhani, M. Almasi, *Thermochim. Acta* 495 (2009) 139–148.
- [71] J. Shaik, M.G. Sankar, D. Ramachandran, C. Rambabu, *J. Solution. Chem.* 43 (2014) 2067–2100.
- [72] V. Alonso, J.A. González, I. García de la Fuente, J.C. Cobos, *Thermochim. Acta* 549 (2012) 246–253.
- [73] C. Moreau, G. Douhéret, *J. Chem. Thermodyn.* 8 (1976) 403–410.
- [74] P. Bordewijk, *Physica* 69 (2) (1973) 422–432.
- [75] JCR. Reis, IM.S. Lampreia, AFS. Santos, MLC.J. Moita, G. Douheret, *Chem. Phys. Chem.* 11 (2010) 3722–3733.
- [76] V. Manjula, T. Vamsi Prasad, K. Balakrishna, K.C. James Raju, T. Vishwam, *J. Mol. Liq.* 299 (2020) 112190.
- [77] T. Vishwam, S. Shihab, V.R.K. Murthy, HaS Tiong, S. Sreehari Sastry, *Spectrochim. Acta, Part A* 179 (2017) 74–82.
- [78] T. Vishwam, K. Parvateesam, S. Sreehari Sastry, V.R.K. Murthy, *Spectrochim. Acta, Part A* 114 (2013) 520–530.
- [79] O. Redlich, A.T. Kister, *Ind. Eng.Chem.* 40 (1948) 345–348.
- [80] H. Eyring, *J. Chem. Phys.* 3 (1935) 107–115.
- [81] T.A. Taha, A. Hassona, S. Elrabaie, M.T. Attia, *J. Asian Ceram. Soc.* (2020) 1–7.
- [82] R. Varadarajan, A. Rajagopal, *Indian J. Pure Appl. Phys.* 36 (1998) 119–124.
- [83] E.R. Lippincott, J.M. Stutman, *J. Phys. Chem.* 68 (1964) 2926–2940.
- [84] A.A. Frost, B. Musulin, *J. Chem. Phys.* 22 (1954) 1017–1020.
- [85] R.J.W. Le Févre, A.J. Williams, *J. Chem. Soc.* (1965) 4185–4188.
- [86] R.G. Parr, W. Yang, *Density-Functional Theory of Atoms and Molecules*, Oxford University Press, New York, 1994.
- [87] A.D. Becke, *J. Chem. Phys.* 98 (1993) 5648–5652.
- [88] C.T. Lee, W.T. Yang, R.G. Parr, *Phys. Rev. B* 37 (1988) 785–789.
- [89] X. Yue, L. Zhao, L. Ma, H. Shi, T. Yang, J. Zhang, *J. Mol. Liq.* 263 (2018) 40–48.
- [90] S.M. Nayeem, M. Kondaiah, K. Sreekanth, M. Srinivasa Reddy, D. Krishna Rao, *J. Therm. Anal. Calorim.* 123 (3) (2016) 2241–2255.
- [91] B.B. Swain, *Curr. Sci.* 54 (1985) 504–506.
- [92] J.H. Espenson, *Chemical Kinetics and Reaction Mechanisms*, 2nd ed., McGraw-Hill, New York, 2002.
- [93] R.J. Sengwa, *Indian J. Pure Appl. Phys.* 41 (2003) 295–300.
- [94] EA. Gomaa, MA. Tahoon, HA. Fawzi, *AASCIT Commun.* 2 (4) (2015) 93–97.
- [95] U.S. Vural, V. Muradoglu, S. Vural, *Bull. Chem. Soc. Ethiop.* 25 (1) (2011) 111–118.
- [96] L.K. Chin, A.Q. Liu, Y.C. Soh, C.S. Lim, C.L. Lin, *Lab. Chip* 10 (2010) 1072–1078.
- [97] RB. Leron, AN. Soriano, M.-H. Li, *J. Taiwan Inst. Chem. Eng.* 43 (2012) 551–557.